Video Article

# Ultrasound Based Assessment of Coronary Artery Flow and Coronary Flow Reserve Using the Pressure Overload Model in Mice

Wei-Ting Chang*[1,2], Sudeshna Fisch*[1], Michael Chen[1], Yiling Qiu[1], Susan Cheng[1], Ronglih Liao[1]

[1]Cardiac Muscle Research Laboratory, Cardiovascular Division, Brigham and Women's Hospital, Harvard Medical School

[2]Division of Cardiovascular Medicine, Chi-Mei Medical Center, Tainan

*These authors contributed equally

Correspondence to: Ronglih Liao at weiting9901@yahoo.com.tw

URL: https://www.jove.com/video/52598
DOI: doi:10.3791/52598

Keywords: Medicine, Issue 98, Coronary flow reserve, Doppler echocardiography, non-invasive methodology, use of animals in research, pressure overload, aortic banding

Date Published: 4/13/2015

Citation: Chang, W.T., Fisch, S., Chen, M., Qiu, Y., Cheng, S., Liao, R. Ultrasound Based Assessment of Coronary Artery Flow and Coronary Flow Reserve Using the Pressure Overload Model in Mice. *J. Vis. Exp.* (98), e52598, doi:10.3791/52598 (2015).

## Abstract

Transthoracic Doppler echocardiography (TTDE) is a clinically useful, noninvasive tool for studying coronary artery flow velocity and coronary flow reserve (CFR) in humans. Reduced CFR is accompanied by marked intramyocardial and pericoronary fibrosis and is used as an indication of the severity of dysfunction. This study explores, step-by-step, the real-time changes measured in the coronary flow velocity, CFR and systolic to diastolic peak velocity (S/D) ratio in the setting of an aortic banding model in mice. By using a Doppler transthoracic imaging technique that yields reproducible and reliable data, the method assesses changes in flow in the septal coronary artery (SCA), for a period of over two weeks in mice, that previously either underwent aortic banding or thoracotomy.

During imaging, hyperemia in all mice was induced by isoflurane, an anesthetic that increased coronary flow velocity when compared with resting flow. All images were acquired by a single imager. Two ratios, (1) CFR, the ratio between hyperemic and baseline flow velocities, and (2) systolic (S) to diastolic (D) flow were determined, using a proprietary software and by two independent observers. Importantly, the observed changes in coronary flow preceded LV dysfunction as evidenced by normal LV mass and fractional shortening (FS).

The method was benchmarked against the current gold standard of coronary assessment, histopathology. The latter technique showed clear pathologic changes in the coronary artery in the form of peri-coronary fibrosis that correlated to the flow changes as assessed by echocardiography.

The study underscores the value of using a non-invasive technique to monitor coronary circulation in mouse hearts. The method minimizes redundant use of research animals and demonstrates that advanced ultrasound-based indices, such as CFR and S/D ratios, can serve as viable diagnostic tools in a variety of investigational protocols including drug studies and the study of genetically modified strains.

## Video Link

The video component of this article can be found at https://www.jove.com/video/52598/

## Introduction

Clinical aortic stenosis (AS) is well known to promote a progressive increase in left ventricular (LV) afterload. To compensate for this chronically rising hemodynamic load, LV hypertrophy (LVH) ensues as an adaptive response[1,2]. The development of LVH is often associated with abnormalities in coronary microcirculation. It is thought that microvascular dysfunction contributes to chronic ischemia in these patients [5]. In addition to coronary flow [3,4], coronary flow reserve (CFR) represents functional change of coronary arteries [1,3] and is defined as the ratio of maximal flow velocity in hyperemia to baseline flow velocity or resting flow velocity[4,6,7]. CFR is decreased during LV remodeling [1-3,5-9] and is used as an index of the extent of functional severity of coronary dysfunction [1,10,17]. It is known to be impaired in many forms of dilated cardiomyopathy [10] and also coronary stenosis[6]. CFR is also a prognostic marker for poor clinical outcomes [12].

LV remodeling in the setting of cardiac dysfunction such as ischemia or LVH is also accompanied by extensive fibrosis, changes in coronary microcirculation and thickening of coronary arteries [1,2]. As a result of these changes in coronary physiology, there is likely remodeling of the coronary arteries. This helps mitigate the effects of low oxygen diffusion and LV diastolic dysfunction that could result in susceptibility to myocardial ischemia [1,2,13].

Genetically modified mice are now a widely prevalent investigational tool for mimicking human disease conditions such as coronary atherosclerosis [5,7,10,12,17]. Particularly the pressure overload model in mice has been widely studied [14,17]. The trans-aortic constriction model (TAC) has been shown to be associated with extensive fibrosis, and coronary stenosis resulting, in part, from medial thickening of coronary arteries and with accompanying changes in coronary flow patterns [1,11,17,19] similar to what is seen in the setting of LVH in humans. While it is

 

known that prolonged pressure overload leads to decompensated heart failure in about 4-8 weeks, the effects on coronary flow dynamics and flow reserve in these models, early in the process of disease progression, and at different stages after banding, are yet to be clearly delineated.

Numerous strains of mice are currently available for research use, including well-characterized LDLR-/- or ApoE-/- mice [10-12], and these have prompted development of sensitive techniques for assessing cardiovascular function and morphology in living mice [11-15]. Such techniques include MRI, PET, contrast CT, high frequency ultrasound, and electron beam tomography [2,9,17,19], all of which provide promising alternatives to invasive methods such as cardiac catheterizations and coronary angiography [12]. However, in mice with very small size of the coronary arteries and high heart rates (HR), imaging of coronary circulation still constitutes a technical challenge for many currently available techniques [4,12]. Interestingly, there has been an exponential rise in technical advances in the field of transthoracic Doppler echocardiography (TTDE), including the development of high-frequency array scan heads with center frequencies from 15 to 50 MHz allowing axial resolutions of approximately 30-100 µm, at depths of 8-40 mm, and frame rates greater than 400 frames-captured/sec. In turn, TTDE-based techniques have emerged as a potentially powerful tool for imaging larger [2] or even smaller vessels such as coronary arteries [5,12].

Another critical advance that has allowed investigators to conduct diagnostic imaging studies of the vasculature in small animals is the carefully controlled use of anesthetics that maintain the heart and respiratory rate of the animals during imaging [11]. Controlled anesthesia maintenance is particularly important for studies related to vasodilation in mice, and the effect of anesthesia also needs to be further explored in this context [10,11]. In humans, on the other hand, TTDE-derived CFR measurements have become a more commonly used tool for evaluation of stenosed and non-obstructed epicardial coronary arteries, predominantly in left anterior descending (LAD) coronary artery [5,16]. However, the prognostic role of CFR and coronary flow changes in asymptomatic patients or mice with preserved LV systolic function at rest has been much less explored [16]. Therefore, the aim of the study was to first establish a clear step-by-step protocol, to evaluate changes in coronary flow using TTDE in a pressure overload mouse model; second, this study examined the prognostic significance of CFR and coronary flow changes in response to pressure overload stress in these mice. We hypothesized that TTDE based assessment of CFR and coronary flow may be useful in the early detection of coronary dysfunction that may precede LV dysfunction.

## Protocol

NOTE: All procedures were performed in mice in accordance with American Veterinary Medical Association (AVMA) guidelines and approved Institutional Animal Care and Use Committees (IACUC) protocols.

## 1. Study Design

1. Use 8-10 week old male C57BL/6 mice (BW~25 g) in the study.
2. Randomize the mice (n = 11) into two groups, the study group selected for aortic banding (n = 8), and the control group (n = 3) to undergo sham operation via thoracotomy.
3. Prepare the animal for imaging by removing hair from the chest using depilatory cream that is medical grade.
4. Perform a first ultrasound (section 2) 24 hr prior to aortic banding to determine baseline parameters at Day -1, between a range of 1% and 2.5% isoflurane (mixed with 100% $O_2$ via nosecone) induced anesthesia.
5. Choose a medically approved anesthetic agent (*i.e.* isoflurane) and monitor the degree of anesthesia (2-3% to induce, and 1.0% to maintain).
   NOTE: Proper anesthesia is crucial in the maintenance of heart beat at normal physiological rates (about 500 beats/min).
6. Confirm the depth of anesthesia by loss of motion from the animal in response to a pedal-withdrawal reflex. Use paralube vet ointment on the eyes to prevent dryness while under anesthesia.
7. Perform surgery at Day 0 [20,21].
8. For aortic banding, ligate the aorta using a 7-0 silk suture around a tapered 26 G needle placed on the arch.
   NOTE: Details regarding the experimental protocol, including the surgical aortic banding procedures, have been described previously [20,21].
9. Perform post-surgery ultrasound imaging (section 2) at Day(s) 2, 6 and 13.
10. Euthanize the mice on Day 14 and harvest the hearts for histological assessment. Euthanize the animals using an overdose of pentobarbital followed by removal of a vital organ such as the heart. Arrest the hearts in diastole and fix with formalin. Use the procedure of the heart harvesting that has been described previously [22].
11. Fix all heart tissues with buffered 10% formalin solution. For trichrome staining, embed tissues in paraffin before sectioning. Use the details of trichrome staining that have been well illustrated previously [14,23].
12. Analyze the data using offline software (section 3).

## 2. Imaging Protocol

1. Long and short axis images of septal coronary artery (SCA) (B- Mode)
   1. Using MS550D probe with center frequency of 40 MHz connected to the active-port, set the application preset to “cardiac imaging”.
   2. With the animal supine on the heated platform, and under anesthesia controlled via nose cone, position the probe using the rail system to obtain the parasternal long axis view (PSLAX) (**Figure 1A**). Always ensure that the animal is kept warm on the prewarmed platform and body temperature is maintained at physiologic levels.
   3. Rotate the probe (with notch pointing caudally) clockwise such that the probe angle is 15° to the left parasternal line (long-axis view) (**Figure 1B**).
   4. Adjust the probe angle by tilting slightly along y axis of the probe to obtain a full-length longitudinal view of the SCA in the center of the screen (**Figure 1B**).
   5. Once the proper landmarks (aortic valve and pulmonary artery) are viewed, cine store the image using the highest frame-rate possible.
   6. By using the “xy” axes micro-manipulators (**Figure 1D**), adjust the probe position to obtain the clearest image of the SCA.
   7. Rotate the probe 90° (with notch pointing caudally) clockwise such that notched end of the probe is to the left of midline (short-axis) (**Figure 1C**).

2. Long and short axis images of SCA (Color-Doppler Mode)
    1. Once a B Mode image is captured or cine-stored, click the color Doppler key on the keyboard to turn on color Doppler acoustic window (**Figure 2**).
    NOTE: This helps to isolate coronary artery (white arrow indicates SCA) either in the long (**Figure 2A**) or in the short axis (**Figure 2C**). Red color is as seen in real time and is indicative of the direction of flow (away from the aortic valve).
    2. Ensure that the focus depth (indicated by a yellow arrowhead on right of the image screen), lies in the center of coronary artery.
    3. Ensure that the data is recorded, using the cine-store key, at the highest possible frame rate (>100 frames/sec).

3. PW Doppler Imaging of SCA (Pulsed-Wave or PW Mode)
    1. While in color-Doppler mode, click on the PW key to bring up a yellow-indicator line on the coronary artery (**Figure 2**, shown in red).
    2. Place the yellow PW line in the middle of the coronary artery in view, at an angle that parallels the directionality of the flow. Note that velocity measurements are highly dependent on the angle of image acquisition.
    3. Adjust the angle of flow (PW angle key) and sample volume (SV key) such that the PW angle key is 60° or less and sample volume captures flow right in the center of the SCA.
    4. Use cine store to capture the wave forms that indicate the velocity of the coronary flow at peak systole (S) and diastole (D) (**Figures 3A** and **3B**), using 1% and 2.5% isoflurane.

## 3. Data Calculation and Analysis

1. Select the velocity time integral (VTI) tool to obtain the peak systolic and diastolic velocities from the images shown in **Figures 3A** and **3B**.
2. Calculate the coronary flow reserve index (CFR) as the ratio of hyperemic (2.5% isoflurane) peak diastolic flow velocity to baseline (1% isoflurane) peak diastolic flow velocity.
3. Calculate the S/D ratio as the peak systolic coronary flow velocity/ peak diastolic coronary flow velocity. Determine the ratio at baseline (1% isoflurane) and at hyperemia (2.5% isoflurane).
4. For standard cardiac function parameters such as FS, FAC, LVM, refer to the manuals from the manufacturer to perform data analysis using proprietary software or refer to Cheng's JoVE paper [2].

## Representative Results

Of the 11 mice that were studied (banded, n=8 and sham, n = 3), adequate and reproducible images were obtained by a single observer at several time-points: at baseline (D-1), D2, D6 and D13. Also, the flow velocity at the constrictive site was measured as 2225 ± 110.9 mm/s, compared with 277.5 ± 10.51 mm/s in the sham mice on the day after the surgery ($p<0.05$). The increase in velocity was the verification of the successful establishment of the pressure overload model. The SCA flow velocity, also referred to here as the CF velocity, the CFR, and the S/D ratios were successfully assessed at baseline and under hyperemia in all mice. Shown in **Figure 3** are CF changes in sham mice under 1% and 2.5% isoflurane. The sham group showed the baseline diastolic CF velocity of ~200 mm/s and hyperemia induced CF velocity of > 600 mm/s. The increase in diastolic CF velocity and was sustained at 13 days in all mice (n = 3, $p >0.05$). Shown in **Figures 3E and 3F** are the CF changes noted in the banded mice, at 1% and at 2.5% isoflurane, respectively. These mice show a similar pattern of induction of hyperemic (2.5%) over baseline (1%) CFvelocity. However, in this group, the diastolic CF velocity showed a dramatic and a systematic reduction over the 14-day evaluation period. Specifically, the diastolic CF velocity in this group was attenuated from 600 mm/s (baseline) to <200 mm/sec (Day 13, post banding). **Figure 4B** summarizes the hyperemic response as seen in CF velocity changes, in the two groups of mice, assessed over 14 days.

CFR is calculated as the ratio of peak diastolic flow velocity in the SCA during maximal vasodilatation induced by 2.5% isoflurane to resting flow velocity under minimal 1% isoflurane. **Figure 4C** summarizes the changes seen in CFR as evaluated in the sham and banded mice. Unlike the sham group, the banded mice showed a marked and continuous decline in the CFR, starting at Day 3 post surgery and persisting through Day 13. This steady reduction in CFR was suggestive of progressive coronary dysregulation causing a reduction in myocardial perfusion, presumably induced by the increase in afterload due to aortic banding ($n = 4$, $p <0.05$). Before banding, average CFR for the mice was calculated as 2.53±0.47 but by 13 days after banding, the CFR in the same mice decreased to 0.59 ± 0.27.

The systolic to diastolic coronary velocity ratio (S/D ratio) represents another indicator of coronary dysfunction. CF essentially occurs during diastole compared to systole. As such, CF in diastole plays a prominent role in maintaining myocardial perfusion [9,15]. It has been reported that distal to the site of coronary stenosis, there is a trend toward an equalization of systolic and diastolic contribution to total CF [17]. Additionally, a significant difference between S/D ratio has been observed between normal and diseased arteries [18]. A cut-off value of S/D ratio as 0.58 was proposed to distinguish between significant and non-significant lesions.

As shown in **Figure 5**, this S/D value increased significantly in the banded group only, both at baseline and in the hyperemic state. There was a significant reduction of diastolic coronary flow velocity after aortic banding. This in part contributed to the elevation of S/D ratio (D0 to D13, 0.45 ± 0.05 to 0.83±0.02 in baseline and 0.27 ± 0.02 to 0.27 ± 0.01 in hyperemic status). As a compensatory mechanism in response to decreased oxygen supply and reduced myocardial perfusion, LV contractility increased, resulting in a concomitant increase of coronary systolic flow velocity (D0 to D13, 89.2 ± 3.2 to 202.5 ± 0.85 mm/sec).

The echo data were benchmarked against histopathological data obtained from the hearts that were harvested at Day 14, from all animals. The latter technique is the current gold standard for coronary function assessment [11]. The hemodynamic parameters evaluated in the study correlated well with histopathological changes in the mouse SCA. As shown in **Figure 6**, Masson's Trichrome staining on the heart sections revealed an increased myocardial and peri-coronary arterial fibrosis in the banded group (n = 4) compared to the sham group (n = 2).

As shown in **Figure 7**, intra- and inter-observer variability was assessed. For intra-observer variability, 20 random waveforms and images for each mouse were selected for repeated measurements that were performed one week apart. There were no significant differences in the peak

velocities measured. For inter-observer variability, two experienced observers evaluated the waveform recordings in a blinded manner. There were no significant differences in the values obtained.

In addition, no significant changes were seen in the traditional echocardiographic parameters used to assess LV function or heart physiology during the 14 days (**Figures 8** and **9**).

Taken together, the results of the study revealed significant changes in coronary circulation in the SCA in all mice. It is also noteworthy that the ultrasound based-changes in CF preceded changes in conventionally assessed LV function, thus reflecting the sensitivity of the method. Although the study was performed on a very small number of mice, results still revealed a high level of significance between the two groups with respect to all pertinent parameters.

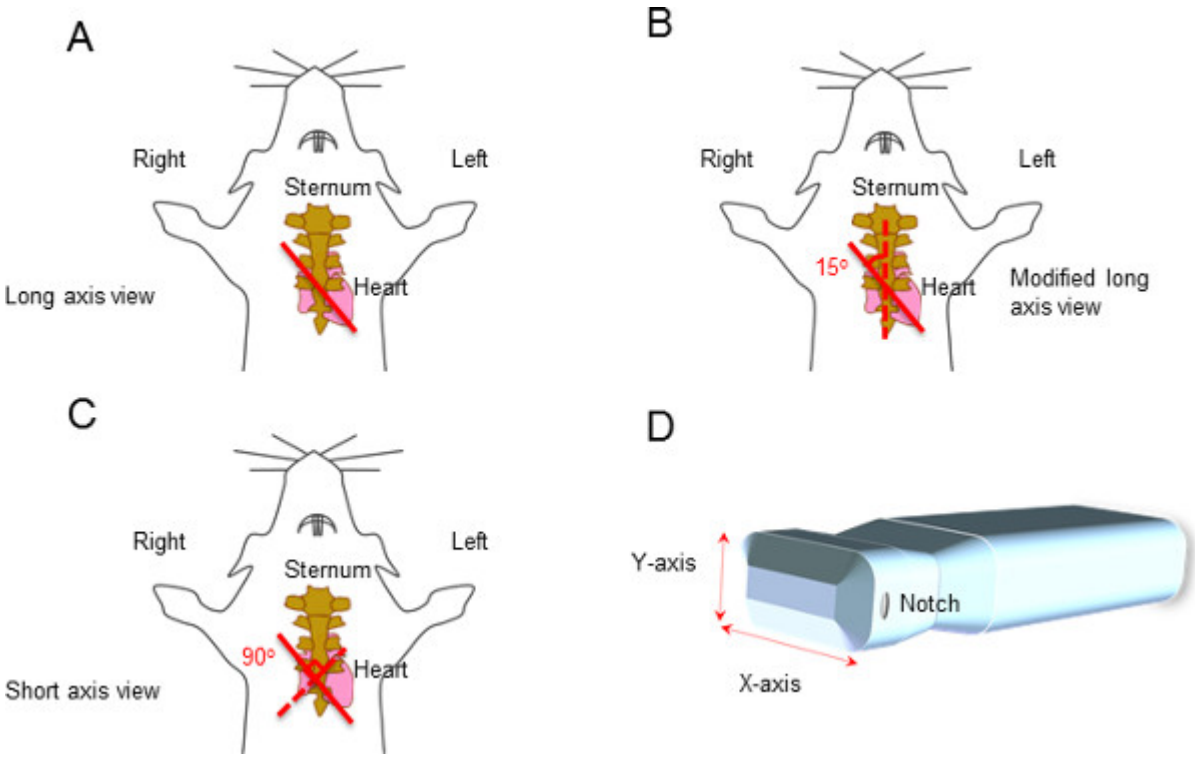


**Figure 1: Ultrasound-based assessment of coronary flow.** The red line indicates the position of the probe for obtaining (**A**) Parasternal long axis (PSLAX) of the heart, and (**B**) Modified parasternal short axis view (mod-PSALX). The dotted like shows that by rotating the probe 15° clockwise from position (**A**), CF can be detected in the SCA, close to aortic sinus and RVOT; (C) Short-axis view (SAX) facilitates imaging of CF using the transverse aortic-level view (**D**) The x-y direction of the probe is indicated.

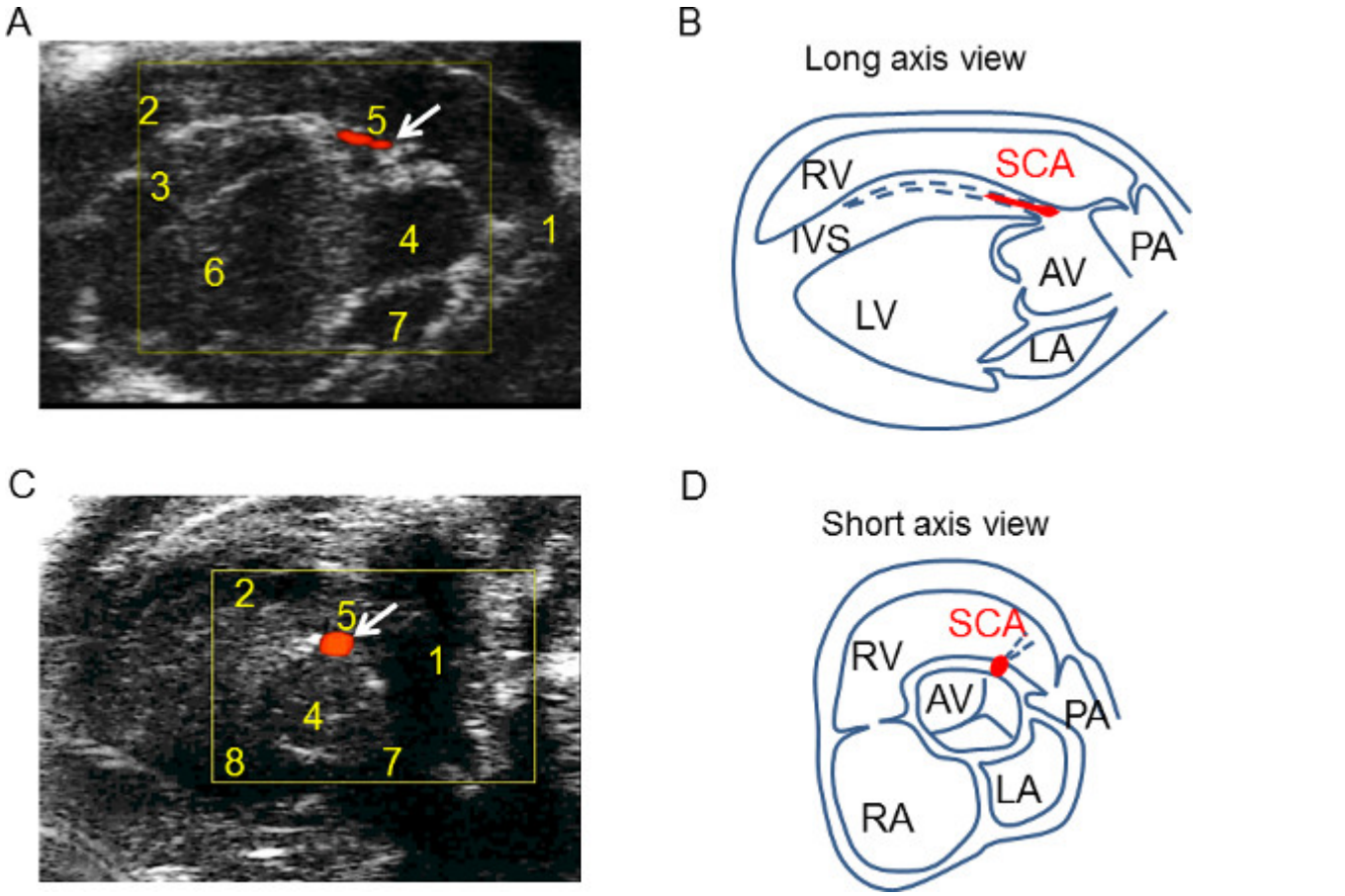


**Figure 2. The coronary flow (CF) detection using the mod-PSLAX and SAX views.** (**A**) The mod-PSLAX view demonstrates CF in the lumen of the SCA parallel to the long axis of the heart, and at 10 o'clock position along the IVS, near AV (**B**) The illustration of mod-PSLAX to indicate the location of SCA and surrounding structures (**C**) The short axis view shows the CF origin from aortic valve toward 1 o'clock position. (**D**) The illustration of short axis view to facilitate the identification of SCA. Key landmarks are in the table of abbreviations.

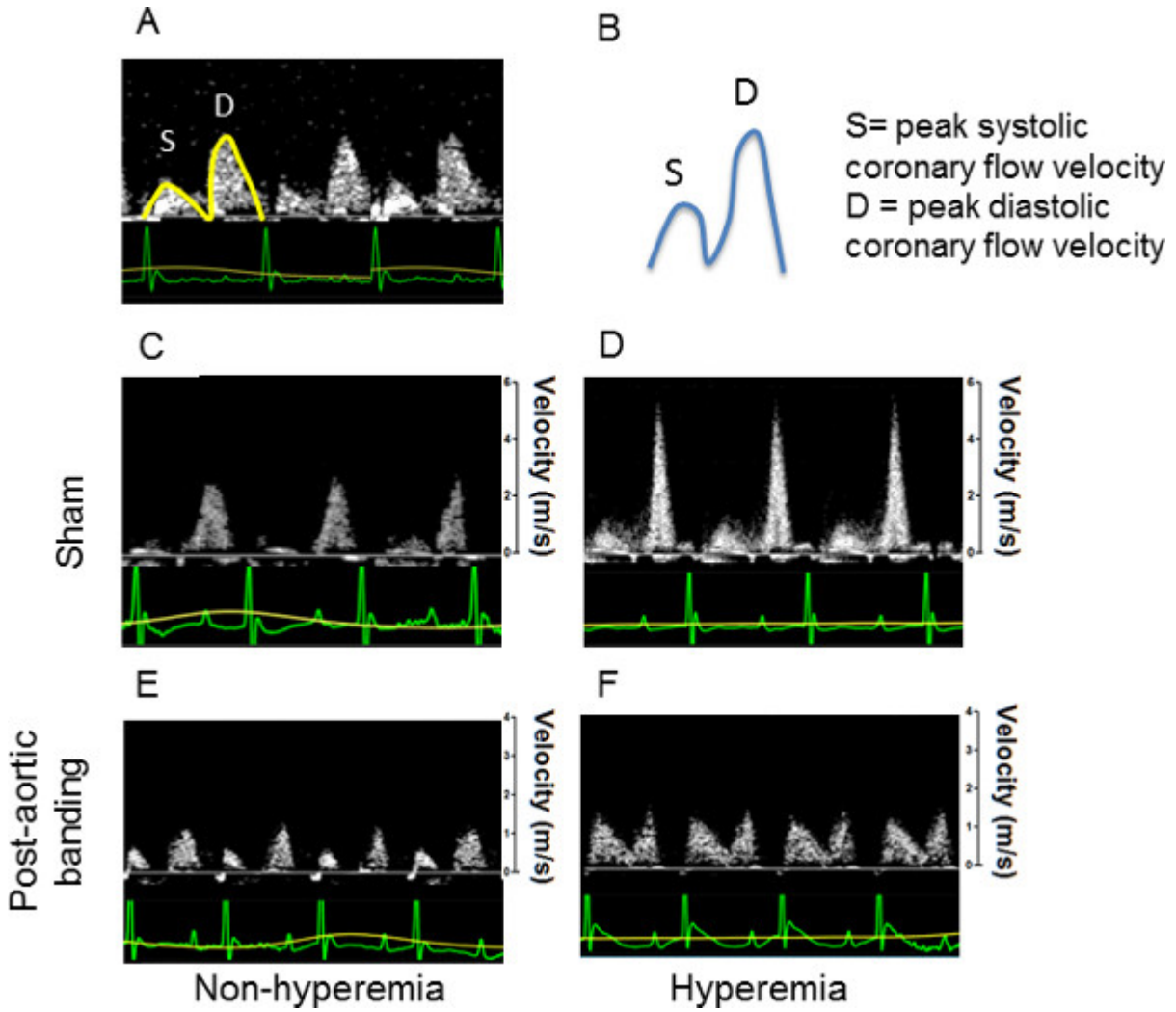


**Figure 3:** Attenuated change of coronary flow (CF) velocity in banded mice under hyperemia compared with Sham (**A**) The yellow line highlights the CF peak in systole (S) and diastole (D). (**B**) The illustration indicates the peak systolic and diastolic flow velocity. Also shown are changes of diastolic CF in the sham mice, under (**C**) 1% and (**D**) 2.5% isoflurane suggesting a hyperemic induction of CF in coronary artery in the sham group. The baseline diastolic CF detected is ~200 mm/sec and rises to >600 mm/sec under hyperemia Changes of diastolic CF in banded mice under (**E**) 1% and (**F**) 2.5% isoflurane. As shown in this group, the changes in (**E**) before and after hyperemia, were similar to the sham group. Following banding, however, (**F**) was markedly attenuated (from 600 m/sec to <200 m/sec), particularly under hyperemia.

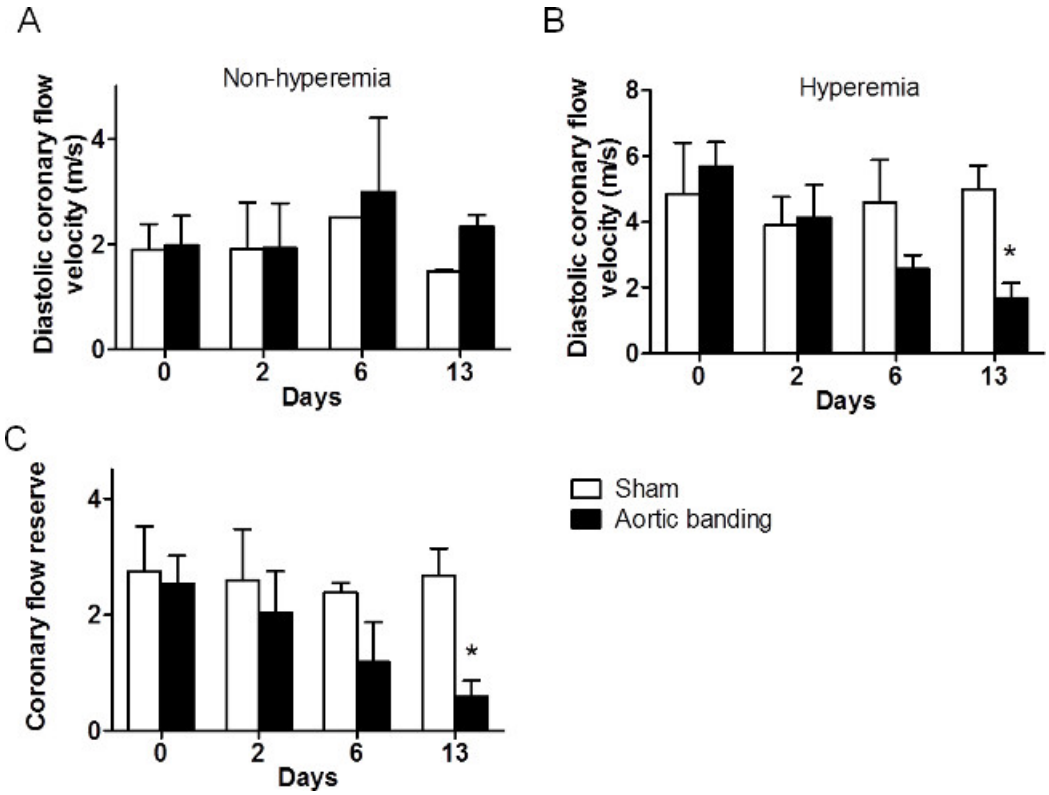


**Figure 4: Comparison of CF velocity and CFR changes in sham and banded mice.** (**A**) CF velocity change in both groups, under 1% isoflurane. The CF was measured as ~200 mm/sec in both sham and banded mice, before hyperemic induction. (**B**) CF velocity change in mice, under 2.5% Isoflurane. The CF velocity was continuously reduced over days following aortic banding. On D13, the CF of sham and banded mice showed significant difference (*: p <0.05). (**C**) Summary of the change in CFR in sham and banded mice. Compared with the sham mice, the CFR of banded mice continuously decreased, correlating with the drop in CF velocity. This phenomenon indicates aortic banding induced increase of afterload and this contributed to coronary dysfunction. (n = 8, *: p <0.05). CFR = $CF_{2.5\%}$ /$CF_{1.5\%}$)

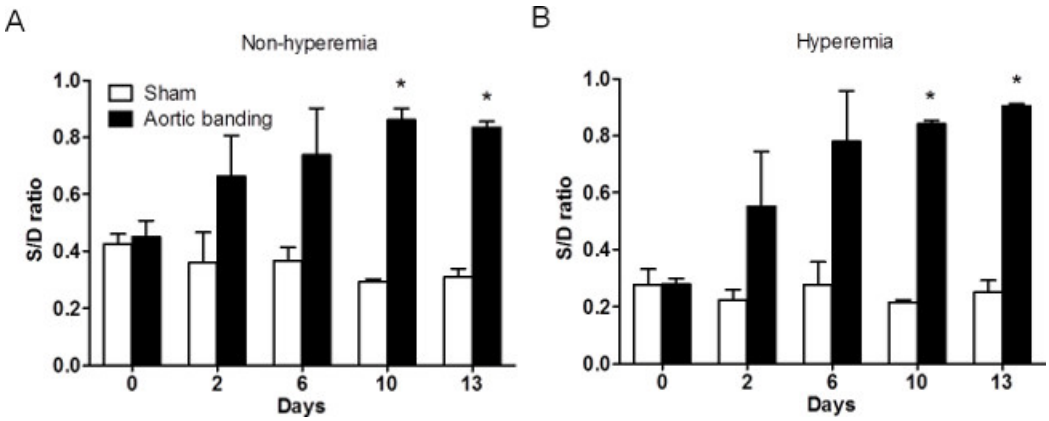


**Figure 5: The change of S/D ratio under 1% and 2.5% isoflurane in sham and banded mice.** (**A**) The change of S/D ratio in both groups at non-hyperemia (1% isoflorane). The S/D ratio increased after surgery and was significant on D9 and D13, even at rest (n = 11, *: p <0.05). (**B**) The change of S/D ratio in both groups under hyperemia (2.5% isoflurane). The S/D ratio also significantly increased after surgery in the hyperemic condition (n = 11, *: p <0.05). S/D = coronary flow velocity in systole/ coronary flow velocity in diastole.

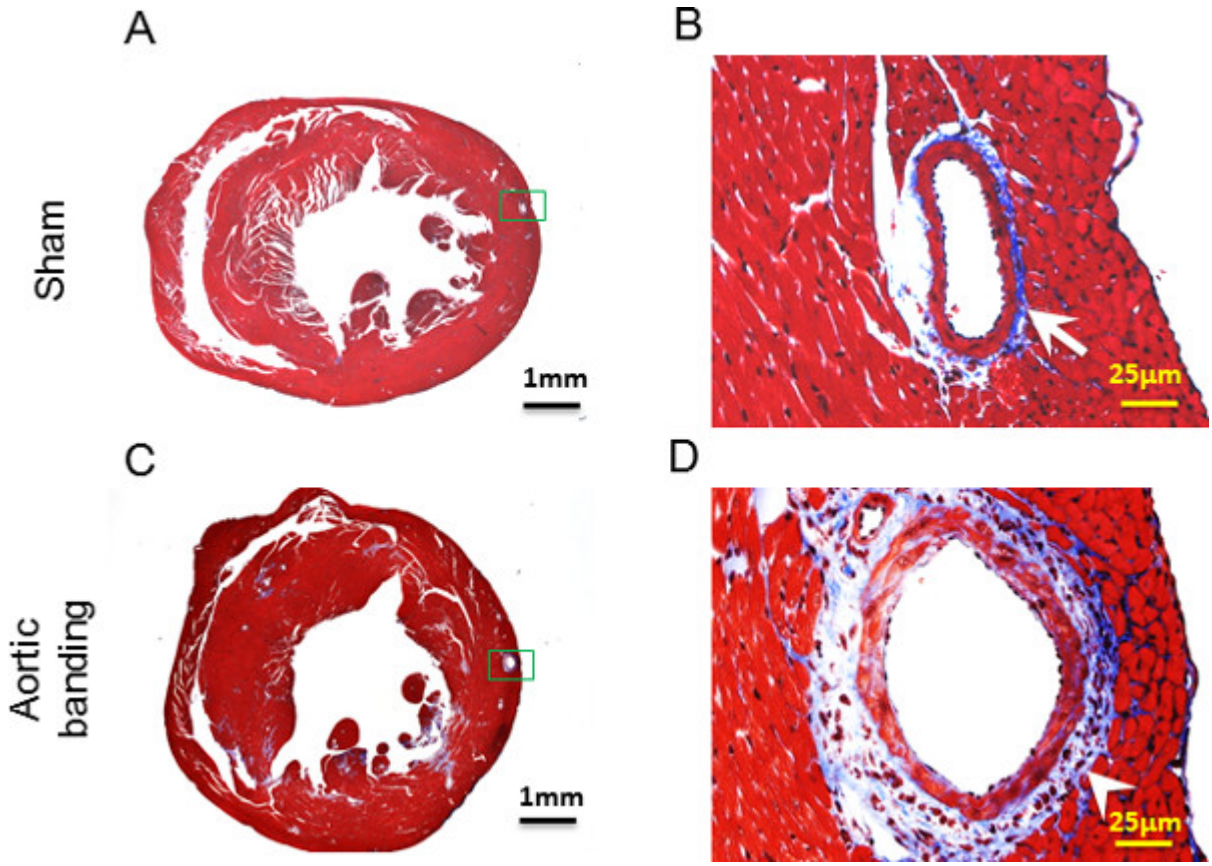


**Figure 6: Myorcardial and pericoronary artery fibrosis detected by Masson Trichrome staining.** Staining was performed in sham and banded mice, two weeks after aortic banding. (**A**) Only limited fibrosis was observed in mid-cavity of the LV in sham mice (20X). (**B**) The images under higher magnification (400X) also showed scant fibrosis around peri-coronary artery area (white arrow indicated fibrosis). (**C**) In the mouse heart following aortic banding, the blue fibrotic area increased significantly (20X). (**D**) Peri-coronary artery fibrosis was also significantly augmented in this group (arrowhead) (X400). The histology data taken together correlate with our echo-based observation of coronary dysfunction.

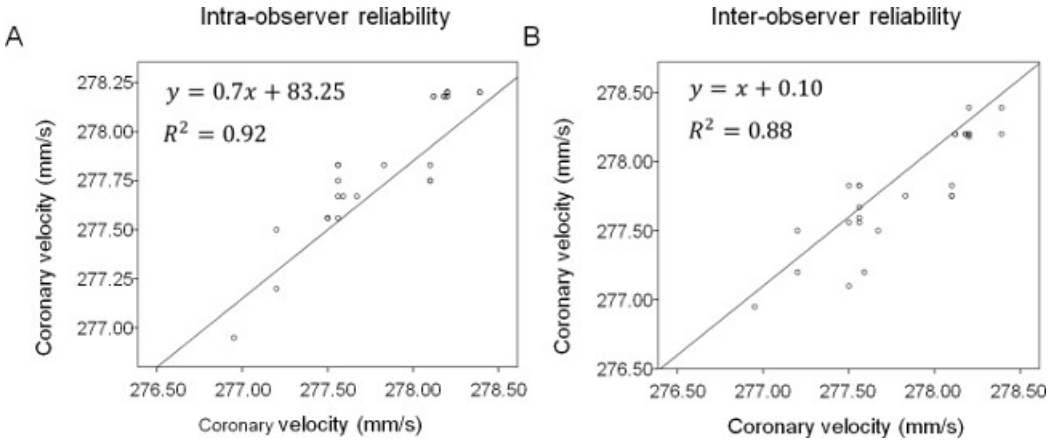


**Figure 7: Intra- and Inter-observer reliability of CF measurement.** (**A**) The intra-observer reliability indicated high a significant correlation ($R^2$ = 0.92). (**B**) The inter-observer reliability also showed high correlation between different observers ($R^2$=0.88).

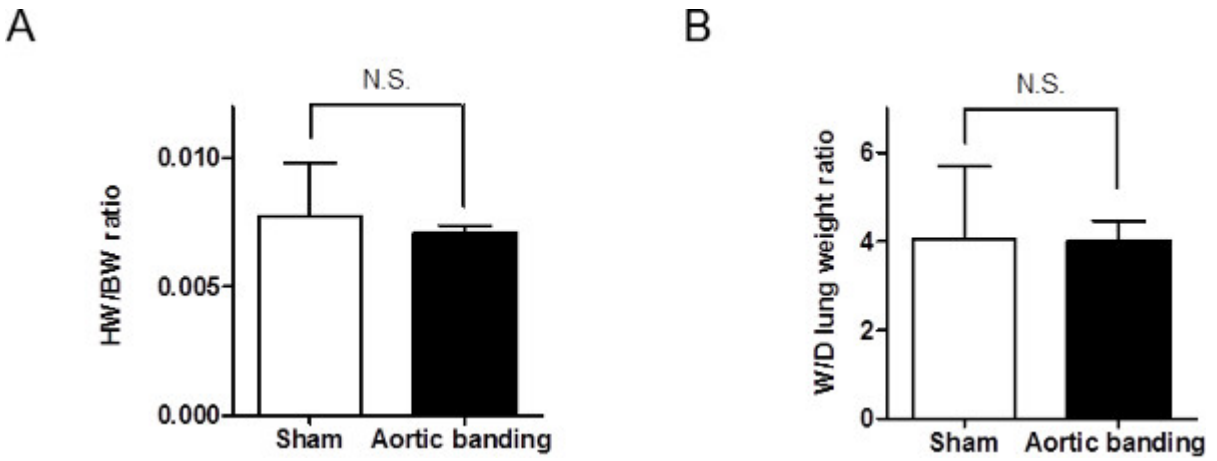


**Figure 8: The heart to body weight (HW/BW) ratio and wet to dry (W/D) lung weight ratio in sham and banded mice.** (**A**) HW/BW ratio was not significantly different between sham and banded mice at Day 15 (n = 11, p >.05). (**B**) The W/D lung ratio was similar in two groups.

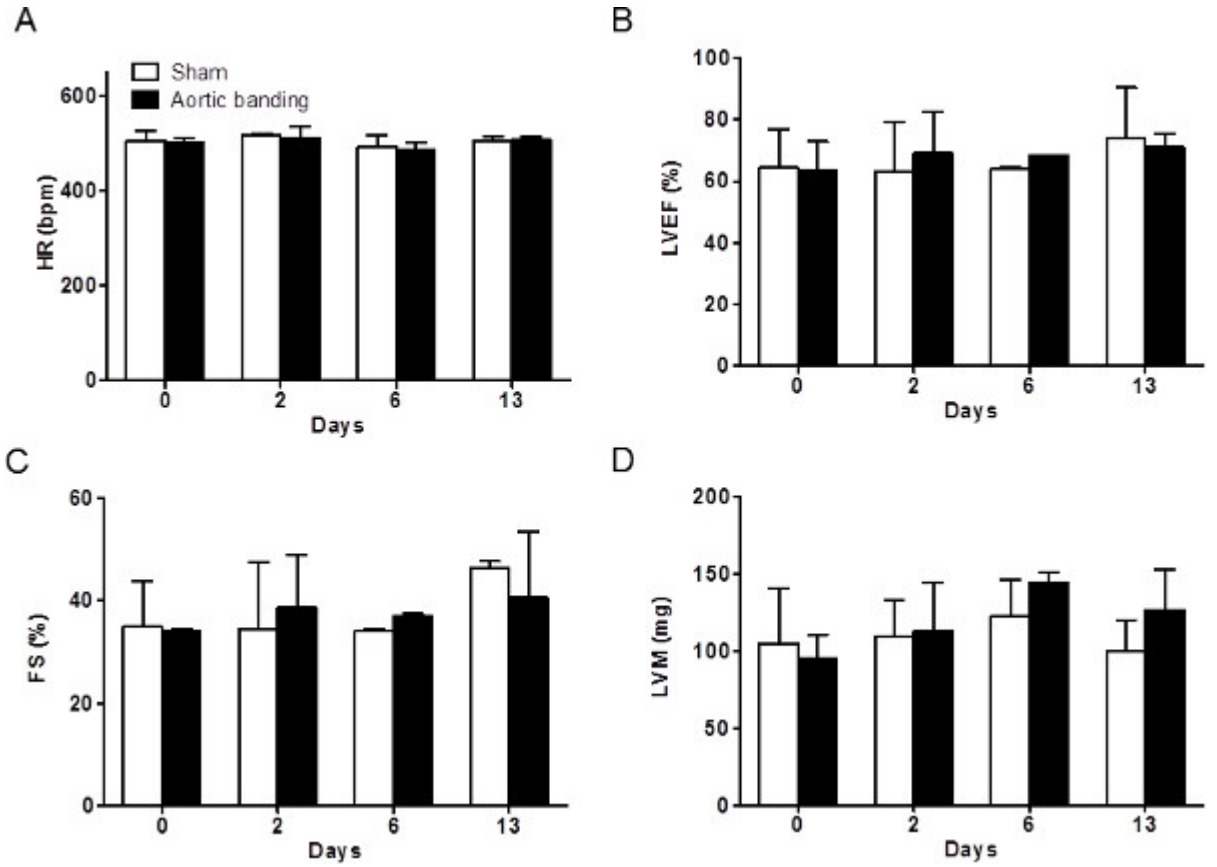


**Figure 9: The heart rate (HR) and conventional echocardiographic parameters.** (**A**) The HR was not significantly changed. As shown in (**B**) left ventricular ejection fraction (LVEF) was not significantly reduced. (**C**) Fractional shortening (FS) was similar in the two groups. (**D**) Left ventricular mass (LVM) did not show significant difference in the two groups, at 13 days post-banding.

| Full name | Abbreviation |
|---|---|
| Aortic stenosis | AS |
| Aortic valve | AV |
| Coronary flow reserve | CFR |
| Congestive heart failure | CHF |
| Fractional shortening | FS |
| Heart rates | HR |

| | |
|---|---|
| Heart to body weight ratio | HW/BW |
| Inter-ventricular septum | IVS |
| Left atrium | LA |
| Left anterior descending | LAD |
| Left coronary artery | LCA |
| Left ventricular ejection fraction | LVEF |
| Left ventricle | LV |
| Left ventricular hypertrophy | LVH |
| Left ventricular mass | LVM |
| Parasternal long axis view | PSLAX |
| Pulmonary artery | PA |
| Right atrium | RA |
| Right ventricle | RV |
| Short-axis view | SAX |
| Septal coronary artery | SCA |
| Systolic to diastolic flow ratios | S/D |
| Transthoracic Doppler Echocardiographic | TTDE |
| Velocity Time Integral | VTI |
| Wet to dry lung weight ratio | W/D |

**Table 1: Abbreviations.**

## Discussion

In this ultrasound based study, non-invasive assessment of coronary flow was reproducibly performed in real time, over days, in live experimental mice; furthermore, the protocol demonstrated the potential to detect coronary artery dysfunction that was present at an early stage and was associated with deficiency in myocardial perfusion. This method could ultimately be leveraged as a clinical tool for cardiovascular risk stratification and/or assessing response to therapeutic intervention.

First, a detailed protocol is described for visualizing the anatomical and functional changes in coronary artery of the small-sized mouse heart, using sequential imaging over time with high frequency color Doppler echocardiography. By carefully pre-selecting a set of complementary acoustic windows with high axial resolution, tightly adjusted sample volume, and proper anesthesia control, any operator (with some training on the ultrasound machine) can perform all the suggested steps of the imaging protocol as well as the post-hoc offline analyses of the acquired data. The method allows reproducible visualization of left main coronary and allows modulation of the visualized coronary function. This protocol can be performed in small animals, such as mice or rats, with high heart and respiration rates. It is possible to obtain reliable data from sequential imaging over days or weeks, which allows investigators to follow function non-invasively and longitudinally in a given experimental model.

Second, the study attempts to evaluate small vessels that are critical to proper cardiac function, by evaluating the small and early changes in intra-coronary physiology (occurring within minutes) within the context of the overall state of cardiac physiology (*e.g.* LV function). The steps of the protocol can be performed in a non-invasive, accurate, and reproducible manner. The measurements obtained in real time can be obtained by any operator with some training on machine operation and basic anatomy. Furthermore, the specific vascular indices measured herein, such as CFR and S/D, can be obtained using any offline measurement software, and not only the proprietary software provided by the machine manufacturer. These indices can be additionally applied to any animal model of interest, such as the ApoE -/- or LDR R-/- models, that can be used to study atherosclerosis. Therefore, the method represents a highly translatable tool for use in studies of a variety of cardiovascular phenotypes.

The novelty of the methodology lies in its agility. It is also easily modifiable by way of minor adjustments such as changing probe placement, choice of probe frequency (highest center-frequency should be picked for low velocity flow assessment such as ischemia studies), sample-volume (smaller sample-volume yield more accurate peak assessment) and angle correction (0° to 60° PW angle, closer to 0° is more accurate), such that any operator can be trained to obtain accurate absolute velocities of the coronary artery, septal or the left-main by following the anatomic landmarks such as PA or aortic root.

Small and temporal changes can be generally hard to measure and can involve a high error rate, related to physiological changes in respiration or heart rate. Troubleshooting usually involves identification of proper landmarks proximal to the origin of the coronary artery and maintenance of normal physiologic heart rate. By monitoring animal physiology using an ECG signal monitoring tool, that is associated with the imaging apparatus, the protocol allows any operator to monitor the effect of any potential vasomodulator (vasoconstrictor or dilator), during imaging.

Proper choice, route and dose of anesthesia levels can be deemed as critical determinants proper estimation of flow dynamics. One limitation of the study could be the use of isoflurane. It is known to cause cardiac depression and change lumen diameter in some studies in a dose

dependent manner [7,10]. However, the images in this study are obtained within minutes, and by using a tightly controlled anesthesia system, one can accurately estimate CF, CFR and S/D at any state of mouse physiology including hypoxia, normoxia, vasodilation, or vascular constriction, with minimal effect of heart rate. Another limitation is the lack of gold standard in correlation between CFR and coronary artery lumen diameter *in vivo* in mice, due to very small sample volume that can be obtained from mice. However, as shown in humans this drawback can be potentially overcome by histologic assessment of coronary morphology with quantitative echocardiography to procure coronary artery diameter [4,24].

By using all the necessary steps outlined in the imaging protocol (Step 2.1.1-2.3.4), CFR and S/D ratio values in mice are obtainable within minutes. High-quality images render the data robust and with low intra- and inter-observer variability.

In summary, the imaging protocol, delineated herein, provides an accurate diagnostic tool representing an alternative to existing invasive options such as coronary catheterization, Doppler-wire or post-mortem histopathologic studies.

Taken together, the findings of this study demonstrate that a non-invasive method of coronary functional assessment as a feasible and viable clinical diagnostic tool that can be used in small animal research. Such a non-invasive method could help to substantially minimize the requirement of animal use, euthanasia, or necropsy in experimental models.

## Disclosures

The authors report no disclosures.

## Acknowledgements

We thank Fred Roberts for exemplary technical support and also appreciate the help from the histology core in Beth Israel Hospital. We thank Brigham Women's Hospital Cardiovascular Physiology Core for providing with the instrumentation and the funds for this work. This work was supported in part by a Department of Medicine Sundry Fund.

## References

1. Yang, F., *et al.* Coronary artery remodeling in a model of left ventricular pressure overload is influenced by platelets and inflammatory cells. *PloS one.* **7**, e40196 (2012).
2. Cheng, H. W., *et al.* Assessment of right ventricular structure and function in mouse model of pulmonary artery constriction by transthoracic echocardiography. *Journal of visualized experiments : JoVE.* e51041 (2014).
3. Meimoun, P., *et al.* Factors associated with noninvasive coronary flow reserve in severe aortic stenosis. *Journal of the American Society of Echocardiography : official publication of the American Society of Echocardiography.* **25**, 835-841 (2012).
4. Bratkovsky, S., *et al.* Measurement of coronary flow reserve in isolated hearts from mice. *Acta physiologica Scandinavica.* **181**, 167-172 (2004).
5. Wu, J., Zhou, Y. Q., Zou, Y., Henkelman, M. Evaluation of bi-ventricular coronary flow patterns using high-frequency ultrasound in mice with transverse aortic constriction. *Ultrasound in medicine & biology.* **39**, 2053-2065 (2013).
6. Hartley, C. J., *et al.* Effects of isoflurane on coronary blood flow velocity in young, old and ApoE(-/-) mice measured by Doppler ultrasound. *Ultrasound in medicine & biology.* **33**, 512-521 (2007).
7. Hartley, C. J., *et al.* Doppler estimation of reduced coronary flow reserve in mice with pressure overload cardiac hypertrophy. *Ultrasound in medicine & biology.* **34**, 892-901 (2008).
8. Saraste, A., *et al.* Coronary flow reserve and heart failure in experimental coxsackievirus myocarditis. A transthoracic Doppler echocardiography study. American journal of physiology. *Heart and circulatory physiology.* **291**, H871-H875 (2006).
9. Scherrer-Crosbie, M., Thibault, H. B. Echocardiography in translational research: of mice and men. *Journal of the American Society of Echocardiography : official publication of the American Society of Echocardiography.* **21**, 1083-1092 (2008).
10. Caiati, C., Montaldo, C., Zedda, N., Bina, A., Iliceto, S. New noninvasive method for coronary flow reserve assessment: contrast-enhanced transthoracic second harmonic echo Doppler. *Circulation.* **99**, 771-778 (1999).
11. Barrick, C. J., Rojas, M., Schoonhoven, R., Smyth, S. S., Threadgill, D. W. Cardiac response to pressure overload in 129S1/SvImJ and C57BL/6J mice: temporal- and background-dependent development of concentric left ventricular hypertrophy. *American journal of physiology. Heart and circulatory physiology.* **292**, H2119-H2130 (2007).
12. Wikstrom, J., Gronros, J., Gan, L. M. Adenosine induces dilation of epicardial coronary arteries in mice: relationship between coronary flow velocity reserve and coronary flow reserve in vivo using transthoracic echocardiography. *Ultrasound in medicine & biology.* **34**, 1053-1062 (2008).
13. Snoer, M., *et al.* Coronary flow reserve as a link between diastolic and systolic function and exercise capacity in heart failure. *European heart journal cardiovascular Imaging.* **14**, 677-683 (2013).
14. Gan, L. M., Wikstrom, J., Fritsche-Danielson, R. Coronary flow reserve from mouse to man--from mechanistic understanding to future interventions. *Journal of cardiovascular translational research.* **6**, 715-728 (2013).
15. Mahfouz, R. A. Relation of coronary flow reserve and diastolic function to fractional pulse pressure in hypertensive patients. *Echocardiography (Mount Kisco, N.Y).* **30**, 1084-1090 (2013).
16. Kawata, T., *et al.* Prognostic value of coronary flow reserve assessed by transthoracic Doppler echocardiography on long-term outcome in asymptomatic patients with type 2 diabetes without overt coronary artery disease). *Cardiovascular diabetology.* **12**, 121 (2013).
17. Miller, D. D., Donohue, T. J., Wolford, T. L., Kern, M. J., Bergmann, S. R. Assessment of blood flow distal to coronary artery stenoses. Correlations between myocardial positron emission tomography and poststenotic intracoronary Doppler flow reserve. *Circulation.* **94**, 2447-2454 (1996).

18. Wada, T., *et al.* Coronary flow velocity reserve in three major coronary arteries by transthoracic echocardiography for the functional assessment of coronary artery disease: a comparison with fractional flow reserve. *European heart journal cardiovascular Imaging.* **15**, 399-408 (2014).
19. Hartley, C. J., *et al.* Doppler velocity measurements from large and small arteries of mice. American journal of physiology. *Heart and circulatory physiology.* **301**, H269-H278 (2011).
20. Almeida, A. C., van Oort, R. J., Wehrens, X. H. Transverse aortic constriction in mice. *Journal of visualized experiments : JoVE.* 1729 (2010).
21. Rockman, H. A., Wachhorst, S. P., Mao, L., Ross, J. ANG II receptor blockade prevents ventricular hypertrophy and ANF gene expression with pressure overload in mice. *American Journal of Physiology.* H2468-H2475 (1994).
22. Virag, J. A., Lust, R. M. Coronary artery ligation and intramyocardial injection in a murine model of infarction. *Journal of visualized experiments : JoVE.* 2581 (2011).
23. Niu, X., *et al.* beta3-adrenoreceptor stimulation protects against myocardial infarction injury via eNOS and nNOS activation. *PloS one.* **9**, e98713 (2014).
24. Ross, J. J., Ren, J. F., Land, W., Chandrasekaran, K., Mintz, G. S. Transthoracic high frequency (7.5 MHz) echocardiographic assessment of coronary vascular reserve and its relation to left ventricular mass. *Journal of the American College of Cardiology.* **16**, 1393-1397 (1990).

 